Natural demodulation of two-dimensional fringe patterns. II. Stationary phase analysis of the spiral phase quadrature transform

Kieran G. Larkin

*Department of Physical Optics, School of Physics, The University of Sydney, Sydney, NSW 2006, Australia, and
Canon Information Systems Research Australia, 1 Thomas Holt Drive, North Ryde, NSW 2113, Australia*

Utilizing the asymptotic method of stationary phase, I derive expressions for the Fourier transform of a two-dimensional fringe pattern. The method assumes that both the amplitude and the phase of the fringe pattern are well-behaved differentiable functions. Applying the limits in two distinct ways, I show, first, that the spiral phase (or vortex) transform approaches the ideal quadrature transform asymptotically and, second, that the approximation errors increase with the relative curvature of the fringes. The results confirm the validity of the recently proposed spiral phase transform method for the direct demodulation of closed fringe patterns. © 2001 Optical Society of America

OCIS codes: 070.2590, 100.2650, 100.5090, 110.6980, 120.2650.

1. INTRODUCTION

This is the second of two papers on the demodulation of two-dimensional (2-D) patterns. In the first paper an isotropic transform was proposed for generating 2-D quadrature functions in a manner analogous to the Hilbert transform (HT) in one dimension.[1] In that publication a number of intriguing historical and conceptual issues were discussed in conjunction with a heuristic description of the method. In this paper we wish to outline the mathematical basis for the quadrature properties of the spiral phase transform. In so doing, we apply the method of stationary phase to a 2-D fringe pattern of quite general form. As far as the author is aware, this powerful method has not been successfully applied to the demodulation and the analysis of fringe patterns before. Stationary phase methods are, however, familiar in the closely related field of computer-generated holograms.[2,3]

The spiral phase transform is closely connected with the 2-D Riesz transform, which is well-known in an area of pure mathematics called harmonic analysis, although little known in physics and engineering. Many papers have been written on the existence and convergence properties of singular integrals such as the Riesz transform, but I have been unable to find any studies that investigate applications in multidimensional demodulation. Furthermore, the inherent deviations from exact quadrature (necessary for exact demodulation) seem to have been overlooked. This paper is an attempt to clarify the approximate quadrature properties of the spiral phase (or vortex) transform by using asymptotic methods.

The initial approach does not directly evaluate the spiral phase transform, because that approach has so far resisted analysis and remains intractable. The analysis has, instead, worked from the other direction by evaluation of (the transform of) the fringe pattern multiplied by an orientational phase factor. The objective then is to show that such a transform asymptotically approaches the fringe transform multiplied by a spiral phase. The one-to-one relation[4,5] of a function and its Fourier transform (FT) then ensures that the direct and indirect approaches are equally valid. This paper is organized as follows. In Section 2 we consider the definition of a 2-D fringe pattern and some methods available for demodulation. In Section 3 we use the method of stationary phase to estimate the FT of a complex fringe pattern and then derive the spiral phase factor. In Section 4 we show that a real fringe pattern can be constructed from two complex-conjugate patterns and (the main result of this paper) that a quadrature relation can be established by using the spiral phase factor. Section 5 reviews the heuristic development of the spiral phase quadrature transform. Section 6 considers an alternative stationary phase expansion that indicates how the spiral phase quadrature relation deviates from the ideal. Section 7 concludes the paper. An appendix on the practical aspects of fringe orientation estimation is included for completeness.

2. TWO-DIMENSIONAL FRINGE PATTERNS

For simplicity, we shall consider a fringe pattern (also known as an amplitude- and frequency-modulated function, or AM–FM function) $f(x, y)$ of the form

$$f(x, y) = b(x, y)\cos[\psi(x, y)] = \frac{b(x, y)}{2}\{\exp[i\psi(x, y)]$$
$$+ \exp[-i\psi(x, y)]\}, \qquad (1)$$

where the offset (or "dc") term of a more general fringe pattern intensity has been removed, also for simplicity.[6] The objective of fringe pattern analysis is to extract both the amplitude and phase modulation terms, $b(x, y)$ and

$\phi(x, y)$, respectively. The amplitude term $b(x, y)$ is more commonly known as the modulation in optical fringe analysis, but to avoid confusion with phase or frequency modulation, it will not be used here. The analysis process is better described in general as 2-D demodulation. One way to demodulate is by estimation of the fringe quadrature component $\hat{f}(x, y)$:

$$\hat{f}(x, y) = -b(x, y)\sin[\psi(x, y)] = -\frac{b(x, y)}{2i}\{\exp[i\psi(x, y)]$$

$$- \exp[-i\psi(x, y)]\}. \qquad (2)$$

In one dimension it is well-known that this quadrature process can be approximated by the HT (the error in the approximation is related to how well the function fits certain band-limit constraints[7]). A significant body of detailed work exists on this subject, and it is covered in a number of standard texts as well as being the basis of the Fourier transform method in fringe analysis.[8] In two (or more) dimensions, the problem requires the definition of a HT analogous to that in the one-dimensional (1-D) case.[9] In most cases this has led to simple extensions based upon separable products of the 1-D HT. Readers interested in previous attempts to extend the HT beyond one dimension are advised to consult Paper I.[1] We shall take as our starting point the idea of a 2-D HT based upon a spiral phase signum function. It is worth noting at this point that iterative methods for 2-D demodulation can give excellent results,[10] although the computational requirements are significant. From the image processing perspective, it is often preferable to have an algorithm that computes the results efficiently through a direct method, if such a method exists. The spiral phase quadrature transform is one such direct method.

3. STATIONARY PHASE EXPANSION OF A COMPLEX PATTERN $p(x, y)$

It is not the objective to give a formal justification of the method of stationary phase. A number of clear, detailed, and rigorous accounts are available. A book by Bleistein and Handelsman contains details of a stationary phase method for multidimensional integrals of Fourier type.[11] Following their approach, we shall initially consider an integral with a complex exponential kernel $p(x, y)$ (analogous to the analytic signal in one dimension[12,13]) and then later separate the real and imaginary parts corresponding to the two quadrature functions:

$$p(x, y) = f(x, y) - i\hat{f}(x, y) = b(x, y)\exp[i\psi(x, y)]. \qquad (3)$$

The 2-D FT is defined as follows:

$$P(u, v) = \int_{-\infty}^{+\infty}\int_{-\infty}^{+\infty} p(x, y)\exp[-2\pi i(ux + vy)]dxdy. \qquad (4)$$

We can write this more compactly as

$$P(u, v) = \int_{-\infty}^{+\infty}\int_{-\infty}^{+\infty} b(x, y)\exp[i\Psi(u, v, x, y)]dxdy, \qquad (5)$$

the total phase function being $\Psi(u, v, x, y) = \psi(x, y) - 2\pi(ux + vy)$. We now parameterize the transform with a factor k that represents a fringe pattern with increasingly close fringes but unchanged envelope:

$$P_k(u, v) = \int_{-\infty}^{+\infty}\int_{-\infty}^{+\infty} b(x, y)\exp[ik\Psi(u, v, x, y)]dxdy. \qquad (6)$$

If we fix on a particular location in frequency space (u, v), then the above equation corresponds to the integral form considered by Bleistein and Handelsman (Ref. 11, p. 340). In this particular case we shall further restrict the functions under consideration to allow us a simple derivation:

- $b(x, y)$ is a real function, continuous, and infinitely differentiable.
- $\Psi(x, y)$ is also a real function, continuous, and infinitely differentiable.

In reality, not all fringe patterns satisfy these constraints. One of the most common exceptions is the branch cut, where the phase $\Psi(x, y)$ has a phase discontinuity but the amplitude $b(x, y)$ is zero. Although such nondifferentiable features are of great practical interest, the stationary phase analysis is less straightforward and is not investigated here. According to Bleistein and Handelsman (Ref. 11, pp. 341 and 380), discontinuities give rise to asymptotic expansions that decay at a slower rate. Figure 1(a) shows an example of a fringe pattern that satisfies the above restrictions. The underlying phase function $\psi(x, y)$ for the depicted fringe pattern is shown in Fig. 1(b). The above restrictions allow us to ignore critical points of the second and third kinds, which would otherwise occur at the edges and the corners of the support boundary. Now we can apply the method of stationary phase directly to Eq. (6), and we find—following Stamnes (Ref. 14, p. 138)—that the result is the sum of contributions from all the critical points:

$$P_k(u_s, v_s) \sim \frac{2\pi}{k}\sum_{n=1}^{N}\frac{\sigma(x_n, y_n)}{|H(x_n, y_n)|^{1/2}}\exp[ik\Psi(x_n, y_n)]$$

$$\times\left[b(x_n, y_n) + \frac{i}{k}Q_2(x_n, y_n)\right], \qquad (7)$$

where the critical points are defined in two dimensions by the phase gradient zeros:

$$\nabla\Psi(x, y) = 0 \Rightarrow \Psi_{1,0}(x, y) = \Psi_{0,1}(x, y) = 0$$

$$\text{at } x = x_n, \ y = y_n. \qquad (8)$$

There is a magnitude term related to the Hessian[15] H of the phase at each critical point, where

$$H(x_n, y_n) = \Psi_{2,0}(x_n, y_n)\Psi_{0,2}(x_n, y_n) - \Psi_{1,1}^2(x_n, y_n), \qquad (9)$$

and the partial derivative of the phase is

$$\Psi_{l,m} = \frac{\partial^{l+m}\Psi}{\partial x^l \partial x^m}. \qquad (10)$$

The factor σ is controlled by the shape of the stationary point:

$$\sigma = \begin{cases} 1 & \text{if } H < 0 \\ i & \text{if } H > 0, \ \Psi_{2,0} > 0 \\ -i & \text{if } H > 0, \ \Psi_{2,0} < 0 \end{cases} \quad (11)$$

Stamnes includes a second-order term Q_2 related to products of various partial derivatives (α_1, α_2, α_3) and the reciprocal of the Hessian:

$$Q_2 = \frac{\alpha_1}{H(x_n, y_n)} + \frac{\alpha_2}{H^2(x_n, y_n)} + \frac{\alpha_3}{H^3(x_n, y_n)}. \quad (12)$$
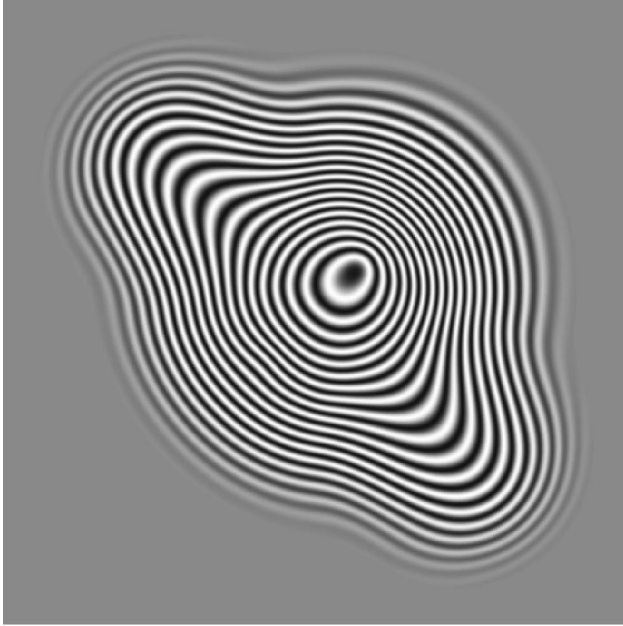
(a)

(b)

Fig. 1. (a) Typical fringe pattern with smooth and differentiable amplitude and phase. (b) Underlying phase function of the fringe pattern in (a). The gray-scale representation has black for 0 rad and white for 70 rad.

Our first-order analysis will ignore this term. We have assumed here that the stationary points (x_n, y_n) are all of lowest order. Higher-order stationarity can be defined, although the expressions become rather complex unless described recursively. Mathematically, this assumption is expressed as

$$H(x_n, y_n) \neq 0. \quad (13)$$

In the case where the stationary points are not isolated, the coefficients will be modified (Papoulis[16] provides a nice example, where a line of points gives a $k^{-1/2}$ rather than a k^{-1} asymptotic coefficient). Again, we shall ignore such complications in the present analysis.

The actual locations of the (isolated) stationary points are related to particular frequencies:

$$\psi_{1,0}(x_n, y_n) = 2\pi u_s, \qquad \psi_{0,1}(x_n, y_n) = 2\pi v_s. \quad (14)$$

We have implicitly considered a Taylor-series expansion around each stationary point:

$$\psi(x_n + s, y_n + t) = \psi_{0,0}(x_n, y_n) + \psi_{1,0}(x_n, y_n)s$$
$$+ \psi_{0,1}(x_n, y_n)t + \frac{\psi_{2,0}(x_n, y_n)s^2}{2}$$
$$+ \frac{\psi_{0,2}(x_n, y_n)t^2}{2} + \cdots, \quad (15)$$

so that

$$\Psi(x_n + s, y_n + t) = \psi_{0,0}(x_n, y_n) + \frac{\psi_{2,0}(x_n, y_n)s^2}{2}$$
$$+ \frac{\psi_{0,2}(x_n, y_n)t^2}{2} + \frac{\psi_{1,1}(x_n, y_n)st}{1}$$
$$+ \cdots. \quad (16)$$

The contribution to the Fourier integral from any one stationary point (x_n, y_n) is

$$[P_k(u_s, v_s)]_n \sim \frac{2\pi}{k} \frac{\sigma(x_n, y_n)}{|H(x_n, y_n)|^{1/2}}$$
$$\times \exp[ik\psi(x_n, y_n)]b(x_n, y_n). \quad (17)$$

Now let us consider another stationary phase expansion of the original fringe pattern, but this time with a slowly varying phase factor $\exp[i\beta(x, y)]$ applied to the amplitude modulation term $b(x, y)$. If the phase factor is suitably slowly varying and differentiable, we can justify this (below we shall consider the alternative of applying it to the phase modulation term). Of particular interest is a phase factor that corresponds to the fringe orientation angle (orientation of steepest phase gradient):

$$\tan[\beta(x, y)] = \frac{\psi_{0,1}(x, y)}{\psi_{1,0}(x, y)}, \qquad 0 \leq \beta < 2\pi. \quad (18)$$

Figure 2(a) shows the general definition of orientation angle from the phase gradient. Figure 2(b) shows the corresponding case for a real fringe pattern. An orientation defined by Eq. (18) is unambiguous in the range 0–2π rad, unlike the orientation of real fringe patterns, where it is not possible to distinguish a fringe from a similar

(a)

(b)
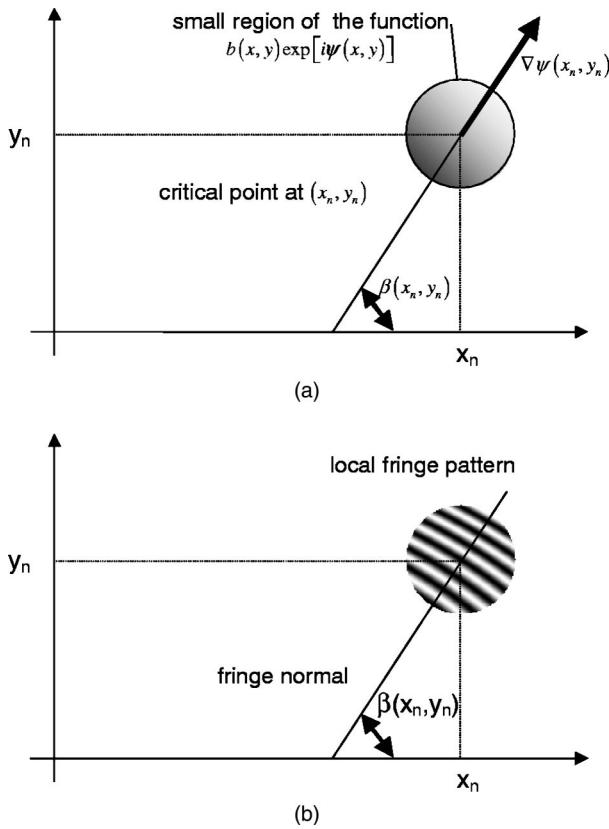
Fig. 2. (a) Definition of orientation angle from the phase gradient. (b) Definition of orientation angle from the fringe angle.

fringe rotated π (in other words, the estimation is mod π). Figure 3(a) shows a gray-scale plot of the orientational phase (mod π) for the fringe pattern in Fig. 1(a). Figure 3(b) shows a gray-scale plot of the orientational phase (mod 2π) for the phase function shown in Fig. 1(b). Readers interested in implementation details are referred to Appendix A, where certain practical aspects of estimating the fringe orientation angle are discussed.

The FT of the fringe pattern modified by $\exp[i\beta(x,y)]$ becomes

$$\tilde{P}_k(u,v) = \int_{-\infty}^{+\infty} \int_{-\infty}^{+\infty} \tilde{b}(x,y)\exp[ik\Psi(u,v,x,y)]\mathrm{d}x\mathrm{d}y,$$
(19)

where the new amplitude $\tilde{b}$ is given by

$$\tilde{b}(x_n,y_n) = b(x_n,y_n)\exp[i\beta(x_n,y_n)]$$

$$= b(x_n,y_n)\frac{\psi_{1,0}(x_n,y_n) + i\psi_{0,1}(x_n,y_n)}{[\psi_{1,0}^2(x_n,y_n) + \psi_{0,1}^2(x_n,y_n)]^{1/2}}.$$
(20)

But, as we have already seen in Eqs. (14), the first-order phase derivatives at isolated stationary points correspond directly to a specific frequency (u_s, v_s); therefore

$$\tilde{b}(x_n,y_n) = b(x_n,y_n)\frac{u_s + iv_s}{\sqrt{u_s^2 + v_s^2}}.$$
(21)

We can define polar frequency coordinates (q, ϕ) by

$$u = q\cos(\phi), \qquad v = q\sin(\phi),$$

$$u_s = q_s\cos(\phi_s), \qquad v_s = q_s\sin(\phi_s);$$
(22)

hence
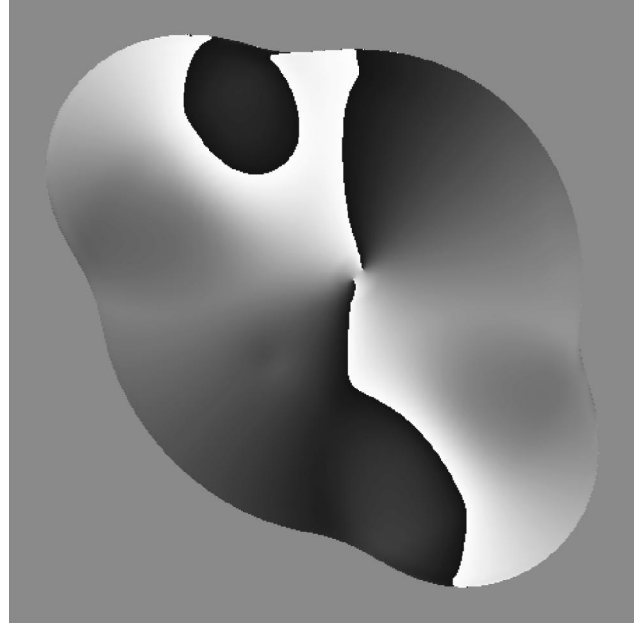
(a)
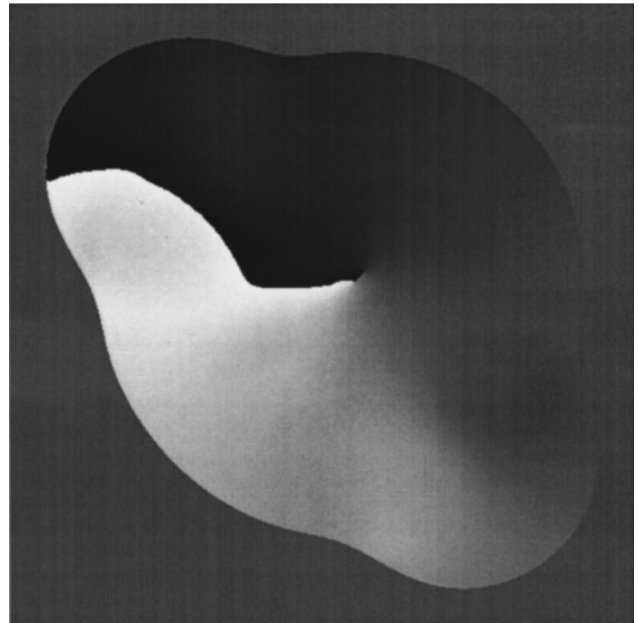
(b)

Fig. 3. (a) Simple square root of orientation phase map (mod π). Gray-scale encoding means that black represents $-\pi/2$ and white represents $+\pi/2$. The singularity occurs at the center of curvature of the closed fringes, where the orientation is undefined. (b) Unwrapped orientation phase map (mod 2π). Gray-scale encoding means that black represents $-\pi$ and white represents $+\pi$. Again, the singularity occurs at the center of curvature of the closed fringes, where the orientation is undefined. Note that the branch cut is not a real (or an imaginary) discontinuity.

$$\tilde{b}(x_n, y_n) = b(x_n, y_n)\frac{u_s + iv_s}{q_s} = b(x_n, y_n)\exp(i\phi_s). \tag{23}$$

The resulting asymptotic approximation is

$$[\tilde{P}_k(u_s, v_s)]_n \sim \frac{2\pi}{k}\frac{\sigma(x_n, y_n)}{|H(x_n, y_n)|^{1/2}}\exp[ik\psi(x_n, y_n)]$$

$$\times b(x_n, y_n)\exp(i\phi). \tag{24}$$

In other words, multiplying a complex exponential pattern $p(x, y)$ in the space domain by an orientational phase factor $\exp[i\beta(x, y)]$ results in a FT that is unaltered except for a spiral phase factor $\exp(i\phi)$ over all frequency space [which has the particular value $\exp(i\phi_s)$ at coordinate (u_s, v_s)]. Relation (24) is a key result of this paper and is a specific instance of the more general result that we wish to demonstrate. The result also applies directly to the complex-conjugate pattern $p^*(x, y)$, which has a reversed orientational phase factor $\exp[-i\beta(x, y)]$ but yields the same Fourier phase factor $\exp(i\phi)$ because the corresponding frequency components rotate 180°. We actually wish to know the result for the complex-conjugate pattern with the original orientational phase factor $\exp[i\beta(x, y)]$:

$$g(x, y) = p^*(x, y) = b(x, y)\exp[-i\psi(x, y)]. \tag{25}$$

The rotated components are

$$[G_k(-u_s, -v_s)]_n \sim \frac{2\pi}{k}\frac{\sigma(x_n, y_n)}{|H(x_n, y_n)|^{1/2}}$$

$$\times \exp[-ik\psi(x_n, y_n)]b(x_n, y_n). \tag{26}$$

Modifying the conjugate pattern by the orientational phase factor yields

$$\tilde{g}(x, y) = p^*(x, y)\exp[i\beta(x, y)]. \tag{27}$$

Finally, its Fourier components are

$$[\tilde{G}_k(-u_s, -v_s)]_n \sim \frac{2\pi}{k}\frac{\sigma(x_n, y_n)}{|H(x_n, y_n)|^{1/2}}\exp[-ik\psi(x_n, y_n)]$$

$$\times b(x_n, y_n)\left(\frac{u_s + iv_s}{\sqrt{u_s^2 + v_s^2}}\right). \tag{28}$$

This can be rewritten with the local spiral phase factor and a sign reversal, the significance of which will become apparent in Section 4:

$$[\tilde{G}_k(-u_s, -v_s)]_n \sim -\frac{2\pi}{k}\frac{\sigma(x_n, y_n)}{|H(x_n, y_n)|^{1/2}}$$

$$\times \exp[-ik\psi(x_n, y_n)]$$

$$\times b(x_n, y_n)\exp[i\phi(-u_s, -v_s)]. \tag{29}$$

4. STATIONARY PHASE EXPANSION OF A FRINGE PATTERN $f(x, y)$

Having derived a result for the complex fringe pattern, we now consider the original real fringe pattern. The cosine term consists of positive and negative phase components. We can use the general relation between the FT of a function and the FT of the complex conjugate of a function, where we denote the FT relation by the symbol $\rightleftharpoons$, so that

$$p(x, y) \rightleftharpoons P(u, v) \Rightarrow p^*(x, y) \rightleftharpoons P^*(-u, -v). \tag{30}$$

Clearly, the FT of the fringe pattern $F(u, v)$ is Hermitian because the fringe pattern $f(x, y)$ is real, and

$$F(u, v) = \frac{P(u, v) + P^*(-u, -v)}{2} = F^*(-u, -v). \tag{31}$$

So the complete FT is composed of two parts, the second of which is obtained by rotating the first by 180° and then conjugating it. In terms of our original stationary phase approximation to $P(u, v)$, we can see that each critical point (x_n, y_n) contributes a component at frequency (u_s, v_s) and a complex-conjugated component at frequency $(-u_s, -v_s)$. In general, the function $P(u, v)$ may occupy a large region of the frequency domain, and hence $P^*(-u, -v)$ is likely to overlap $P(u, v)$ significantly. This overlap is the source of the difficulty that Fourier-based methods have in analyzing closed fringe patterns. Masks simply cannot separate overlapping components in the Fourier domain. Something more subtle than masking is required.

We now consider the real fringe pattern modified by the orientational phase factor

$$\tilde{f}(x, y) = \tilde{b}(x, y)\cos[\psi(x, y)]$$

$$= \frac{b(x, y)}{2}\exp[i\beta(x, y)]$$

$$\times \{\exp[i\psi(x, y)] + \exp[-i\psi(x, y)]\}. \tag{32}$$

The orientational phase factor here is the mod 2π form (see Appendix A) simultaneously applied to both positive and negative exponential components of the fringe pattern. Applying the FT and considering only those components at the two diametrical frequencies (u_s, v_s) and $(-u_s, -v_s)$ that are due to the stationary phase critical points at (x_n, y_n) previously defined in Section 3 [relations (24) and (29)], we find that

$$2\tilde{F}_{s,n}(u, v) \approx [\tilde{P}_k(u_s, v_s)]_n\delta(u - u_s, v - v_s)$$

$$+ [\tilde{P}_k(-u_s, -v_s)]_n\delta(u + u_s, v + v_s). \tag{33}$$

Expanding the terms gives

$$2\tilde{F}_{s,n}(u,v) \sim \frac{2\pi}{k} \frac{\sigma(x_n,y_n)}{|H(x_n,y_n)|^{1/2}} b(x_n,y_n)\exp[i\phi(u_s,v_s)]$$

$$\times \{\exp[ik\psi(x_n,y_n)]\delta(u-u_s,v-v_s)$$

$$-\exp[-ik\psi(x_n,y_n)]\delta(u+u_s,v+v_s)\}. \quad (34)$$

The above equation is recognizable as the FT of a quadrature fringe pattern (that is to say, a sine pattern rather than a cosine pattern) multiplied by a spiral phase factor. In particular, if we have a real fringe pattern $w(x,y)$ defined by

$$w(x,y) = b(x,y)\sin[\psi(x,y)], \quad (35)$$

then we can easily show, by using the preceding methods, that the FT components that are due to the stationary point (x_n,y_n) are

$$2iW_{s,n}(u,v) \sim \frac{2\pi}{k} \frac{\sigma(x_n,y_n)}{|H(x_n,y_n)|^{1/2}} b(x_n,y_n)$$

$$\times \{\exp[ik\psi(x_n,y_n)]\delta(u-u_s,v-v_s)$$

$$-\exp[-ik\psi(x_n,y_n)]\delta(u+u_s,v$$

$$+v_s)\}. \quad (36)$$

Combining relations (34) and (36), we find that

$$2\tilde{F}_{s,n}(u,v) = 2iW_{s,n}(u,v)\exp[i\phi(u_s,v_s)]. \quad (37)$$

In other words, applying the orientational phase function to the real fringe pattern f corresponds to a multiplication by a spiral function in the Fourier domain. The Fourier multiplication applies to the FT of the fringe quadrature function. Without loss of generality, the spiral phase can be considered to apply over the full Fourier plane, not just at the two diametrical frequencies. The complete FT expression is to be formed by summing (integrating) the contributions from all critical points because the process is additive (all points with the same β result in Fourier components at the same polar angle ϕ).

The overall process in Eq. (37) can be summarized in operator notation, with $\mathcal{F}\{\}$ and $\mathcal{F}^{-1}\{\}$ representing the forward and inverse FT operators, respectively:

$$\mathcal{F}\{\exp(-i\beta)b\cos(\psi)\} \sim \exp(i\phi)\mathcal{F}\{ib\sin(\psi)\}. \quad (38)$$

The spiral phase transform proposed here can be succinctly expressed by the inverse FT of relation (38).

$$\mathcal{F}^{-1}\{\exp(i\phi)\mathcal{F}\{b\sin(\psi)\}\} \sim -i\exp(i\beta)b\cos(\psi). \quad (39)$$

The result is to be considered asymptotically correct in the sense of a first-order stationary phase expansion of a function containing only critical points of the first kind. If instead we had started with a quadrature fringe pattern, then we would have obtained the following relations (by setting $\psi = \psi' + \pi/2$):

$$\mathcal{F}^{-1}\{\exp(i\phi)\mathcal{F}\{b\cos(\psi')\}\} \sim +i\exp(i\beta)b\sin(\psi'). \quad (40)$$

Finally, we have arrived at the result called here the "spiral phase quadrature transform" or vortex transform, $V\{\}$, for short:

$$b\sin(\psi) \sim -i\exp(-i\beta)\mathcal{F}^{-1}\{\exp(i\phi)\mathcal{F}\{b\cos(\psi)\}\}$$

$$= \mathcal{V}\{b\cos(\psi)\}. \quad (41)$$

Relation (41) is the main result of this paper. Relation (41) represents a direct and efficient method for estimating the quadrature component of a quite general 2-D fringe pattern and is therefore a natural method of 2-D demodulation. The transform can be performed optically with just two phase-only holograms, in a manner reminiscent of a general coordinate transformation using multiple holographic elements.[3] There are indications that the second-order term appearing in Eq. (12) is also consistent with the spiral phase result in relation (41), but the analysis is not pursued here. Interestingly, relation (41) can be extended to higher- (integer-) order spirals, where only the odd orders have the quadrature property.

5. HEURISTIC DEVELOPMENT OF THE SPIRAL PHASE QUADRATURE TRANSFORM

The preceding derivations have been, by necessity, rather circuitous and nonintuitive. Our stationary phase theory was developed quite some time after we had discovered the vortex transform experimentally. In turn, the experimental discovery was prompted by a number of heuristic arguments for the essential features of a 2-D quadrature transform outlined in our initial expository work.[1]

The essential heuristic reasoning follows. We can see from Fig. 2(b) that each region in the interferogram has a well-defined fringe orientation (β_0) and spacing. The stationary phase method allows us to consider components that contribute to the FT from each such region (at a pair of diametrically opposed frequencies). If we multiply the FT by a pure spiral phase factor, then the polarity of these components at opposite frequencies is flipped (because the phase spiral is an odd function) while each maintains the fixed phase factor $\exp(i\beta_0)$. Calculating the inverse FT now gives a quadrature function with an orientational phase factor $\exp(i\beta_0)$, which can be neutralized if we know (or can estimate) the local fringe orientation. Note that the orientation should be mod 2π because we originally assume it to be defined by the gradient of the phase derivative without any sign-related ambiguities. In essence, the stationary phase method allows us to consider a small region of the complex "analytic" image[12] underlying the interferogram and then let the number of fringes in that region tend to infinity. This results in the relative curvature of the fringes diminishing (here the relative curvature is defined as the fringe spacing divided by the radius of curvature), so that the fringes are effectively straight and contribute only to a single frequency component determined by the phase gradient.

6. ERROR ANALYSIS FOR THE STATIONARY PHASE EXPANSION OF A COMPLEX PATTERN $p(x,y)$

In Section 3 we considered the stationary phase expansion of an integral with an orientational phase factor

$\exp(i\beta)$ applied to the amplitude function. The justification for this is that the factor is slowly varying. If, however, we consider the factor to be of significant variation, then we should really include it in the rapidly varying phase part. This approach is appropriate for patterns with widely spaced fringes or tightly curved fringes. In this section we will discover the implications of modifications to the phase part.

The integral that we shall consider is similar to that in Section 3, Eq. (6):

$$\check{P}_k(u,v) = \int_{-\infty}^{+\infty}\int_{-\infty}^{+\infty} b(x,y)\exp\{k[i\Psi(u,v,x,y)$$
$$- i\beta(x,y)]\}dxdy. \qquad (42)$$

The diacritic in the function $\check{P}_k$ is used to indicate that an alternative stationary phase expansion has been used. It is worth considering what this integral means physically as the parameter k tends to infinity. In Section 3 the orientational phase is independent of k, and the limit represents a single spiral acting on a fringe pattern with very finely spaced fringes. In this section we have the orientational phase increasing as the fringe spacing decreases. This means that the orientational phase component maintains the same strength relative to the fringe pattern phase, so that relative error effects are maintained as k tends to infinity. The stationary phase expansion is

$$[\check{P}_k(\check{u}_s,\check{v}_s)]_n \sim \frac{2\pi}{k}\frac{\check{\sigma}(\check{x}_n,\check{y}_n)}{|\check{H}(\check{x}_n,\check{y}_n)|^{1/2}}$$
$$\times \exp[ik\Psi(\check{x}_n,\check{y}_n)]b(\check{x}_n,\check{y}_n). \quad (43)$$

Again the ˘ mark above the symbols is used to indicate that the alternative expansion maps (modified) critical point contributions at $(\check{x}_n,\check{y}_n)$ to modified frequency coordinates $(\check{u}_s,\check{v}_s)$. The essential change occurs in the stationary point conditions because the orientational phase has a nonzero gradient, which induces a shift in the overall phase gradient. The overall phase function is

$$\Psi(u,v,x,y) = \psi(x,y) - 2\pi(ux + vy) - \beta(x,y). \qquad (44)$$

The stationary point conditions are determined by the null gradient

$$\nabla\Psi(\check{u}_s,\check{v}_s,\check{x}_n,\check{y}_n) = 0. \qquad (45)$$

The shift in the frequencies is more explicitly shown by

$$\psi_{1,0}(\check{x}_n,\check{y}_n) - \beta_{1,0}(\check{x}_n,\check{y}_n) = 2\pi\check{u}_s = 2\pi(u_s - \Delta u_s),$$
$$\psi_{0,1}(\check{x}_n,\check{y}_n) - \beta_{0,1}(\check{x}_n,\check{y}_n) = 2\pi\check{v}_s = 2\pi(v_s - \Delta v_s). \qquad (46)$$

Using the original definition of the fringe orientation as the direction of the initial phase gradient, we find that

$$2\pi\Delta u_s = \beta_{1,0} = \frac{\psi_{1,0}\psi_{1,1} - \psi_{0,1}\psi_{2,0}}{\psi_{1,0}^2 + \psi_{0,1}^2}$$
$$= \frac{u_s\psi_{1,1} - v_s\psi_{2,0}}{2\pi q_s^2},$$

$$2\pi\Delta v_s = \beta_{0,1} = \frac{\psi_{1,0}\psi_{0,2} - \psi_{0,1}\psi_{1,1}}{\psi_{1,0}^2 + \psi_{0,1}^2}$$
$$= \frac{u_s\psi_{0,2} - v_s\psi_{1,1}}{2\pi q_s^2}. \qquad (47)$$

This means that the frequency shift that is due to the orientational phase factor is exactly zero if and only if $\beta_{0,1} = \beta_{1,0} = 0$. This can occur only if the Gaussian curvature or the Hessian H of the underlying phase function is zero:

$$\psi_{2,0}\psi_{0,2} - \psi_{1,1}^2 = 0. \qquad (48)$$

This is then a necessary, but not a sufficient,[17] condition. In effect, this means that frequency shifts that are due to the orientational phase will not occur in regions where the fringes are locally straight (i.e., not changing orientation with position). Earlier, we excluded such (straight) regions from the patterns considered in our analysis to avoid higher-order evaluations of the parameter H. Regions where the Hessian is zero are known to correspond to catastrophes (or caustics) in the focusing of light. Figure 4 shows a gray-scale representation of the magnitude of the Hessian of the phase function shown in Fig. 1(b). A number of curves are visible with low values of $|H|$. In the book by Nye,[18] Eq. (2.10) corresponds directly with our condition in Eq. (48) above. The main difficulty with catastrophes is the singularity in the Fourier amplitude so introduced. Incorporation of catastrophes (also equivalent to the merging of multiple stationary points) in our stationary phase analysis is possible but may be expected to make many of the important derivations lengthy and complicated. In this publication we shall consider only fringe patterns with isolated (interior) stationary points. This then implies that there is always a
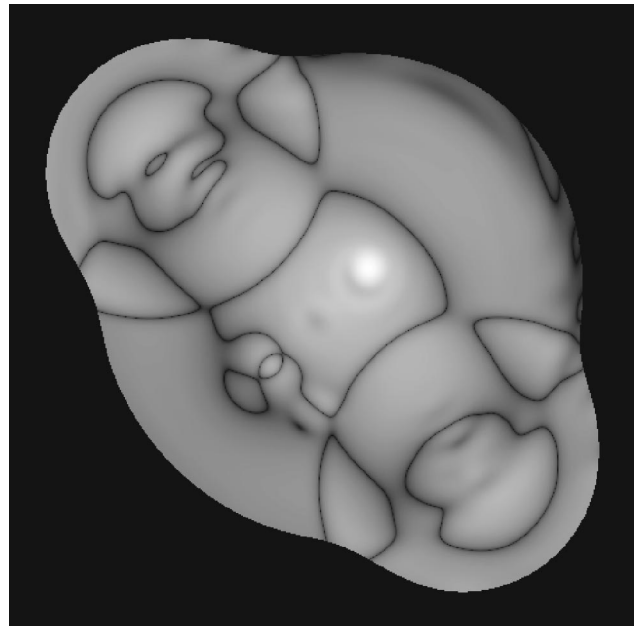
Fig. 4. Magnitude of the Hessian of the phase. Gray-scale encoding means that black represents zero and white represents peak value. The magnitude has been set to zero in the outer region, where the fringe amplitude is insignificant.
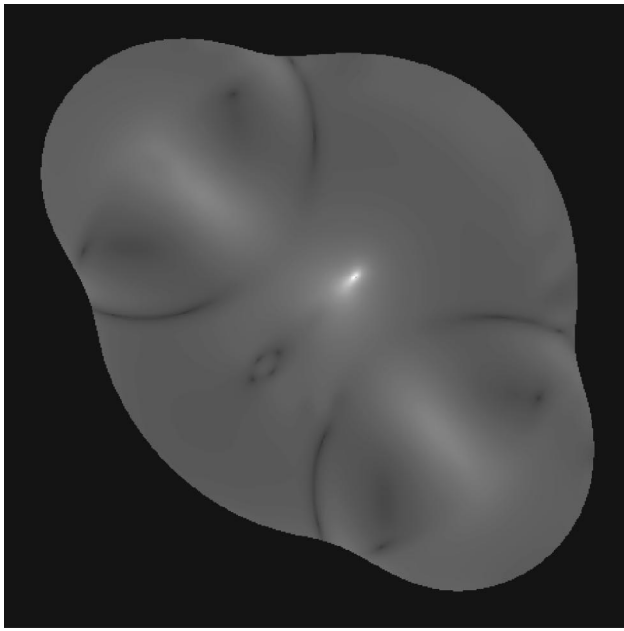
(a)
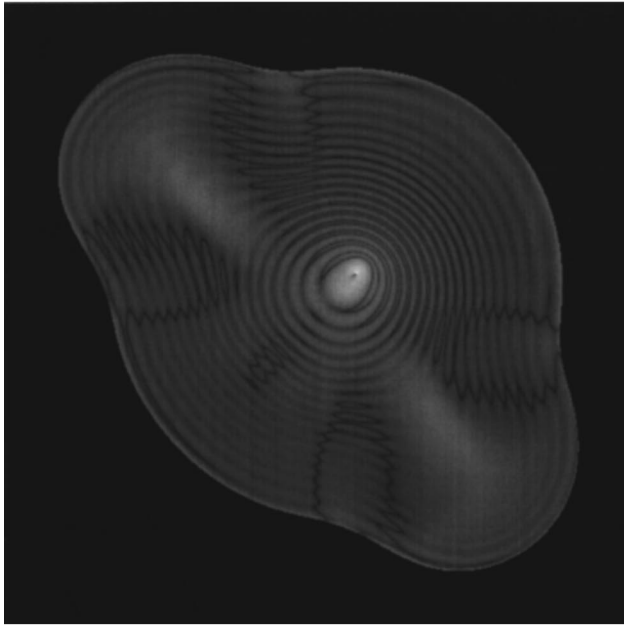
(b)

Fig. 5. (a) Sixth root of the magnitude of the relative curvature of the phase. Gray-scale encoding means that black represents zero and white represent peak value (152, dimensionless units). The magnitude has been set to zero in the outer region, where the fringe amplitude is insignificant. The sixth root is chosen to emphasize certain features. Note that the rms value (excluding the region within one fringe of the central discontinuity) is 0.029. (b) Sixth root of the magnitude of actual error in the phase derived by using the vortex operator on the fringe pattern of Fig. 1. Gray-scale maximum (white) is 2.6 rad, and the minimum (black) is 0.0 rad.   Note that the rms phase value (excluding the region within one fringe of the central discontinuity) is 0.017 rad.

frequency shift (that is due to the orientation phase gradient) for the patterns under consideration. The frequency shift means that we now have a frequency component at $(u_s - \Delta u_s, \; v_s - \Delta v_s)$ with a phase $k[\psi(\check{x}_n, \check{y}_n)$

$-\beta(\check{x}_n, \check{y}_n)]$. We expect that this frequency shift will introduce a discrepancy between the ideal spiral Fourier phase and the actual phase contribution through the stationary phase. Comparing this with a kth-order spiral phase in the Fourier domain is possible if we estimate the rotation $\Delta \phi$ caused by the frequency shift:

$$\tan(\phi + \Delta \phi) = \tan\left(\frac{v_s - \Delta v_s}{u_s - \Delta u_s}\right). \tag{49}$$

We can use the error propagation property of the arctangent[19] to find a small-angle error approximation

$$\Delta \phi \simeq \frac{u_s \Delta v_s - v_s \Delta u_s}{u_s^2 + v_s^2}, \qquad (\Delta u_s)^2 \ll u_s^2 + v_s^2,$$

$$(\Delta v_s)^2 \ll u_s^2 + v_s^2. \tag{50}$$

Using the above values for these parameters, we obtain

$$\Delta \phi \simeq \frac{\psi_{1,0}^2 \psi_{0,2} + \psi_{0,1}^2 \psi_{2,0} - 2\psi_{1,0}\psi_{0,1}\psi_{1,1}}{(\psi_{1,0}^2 + \psi_{0,1}^2)^2}$$

$$= \frac{\psi_{1,0}^2 \psi_{0,2} + \psi_{0,1}^2 \psi_{2,0} - 2\psi_{1,0}\psi_{0,1}\psi_{1,1}}{(\psi_{1,0}^2 + \psi_{0,1}^2)^{3/2}} \frac{1}{(\psi_{1,0}^2 + \psi_{0,1}^2)^{1/2}}. \tag{51}$$

The above formula may be recognized as the curvature of a 2-D function ψ [see Granlund and Knutsson (Ref. 20, p. 361, for example)] divided by the magnitude of the gradient. We have seen errors apparently following the relative curvature in experimental testing of the spiral phase algorithm. The above result indicates that the proportionality constant is simply unity. In paper I [Ref. 1, relation (28)], we determined the second-order error in the estimated phase that is due to an error in the orientation phase ϵ. In a similar manner we expect that the error in the estimated phase $\delta\psi$ can be determined from $\delta\phi$, the spiral phase error in relation (51). However, the particulars of the error propagation (especially first- and second-order error cancellation) are dependent upon the detailed implementation of the vortex operator, including the orientation estimator. Only the qualitative structure of the curvature-induced error is considered here. Figure 5(a) shows a gray-scale representation of the relative curvature function in relation (51). Figure 5(b) is a gray-scale representation of the actual phase error arising from vortex operator demodulation. Apart from the residual fringe structure in Fig. 5(b), the two figures are broadly consistent, especially regarding the location of extrema.

The frequency shifting gives rise to a phase error when compared with the Fourier spiral phase. Another effect is related to the amplitude change that is due to the Hessian at the critical point, given by

$$\check{H}(\check{x}_n, \check{y}_n) = \check{\Psi}_{0,2}(\check{x}_n, \check{y}_n)\check{\Psi}_{2,0}(\check{x}_n, \check{y}_n) - \check{\Psi}_{1,1}^2(\check{x}_n, \check{y}_n)$$

$$= (\psi_{0,2} - \beta_{0,2})(\psi_{2,0} - \beta_{2,0}) - (\psi_{1,1} - \beta_{1,1})^2$$

$$= H(\check{x}_n, \check{y}_n) + (\beta_{2,0}\beta_{0,2} - \beta_{1,1}^2) - (\psi_{0,2} - \beta_{2,0}$$

$$+ \psi_{2,0}\beta_{0,2} - 2\psi_{1,1}\beta_{1,1}). \tag{52}$$
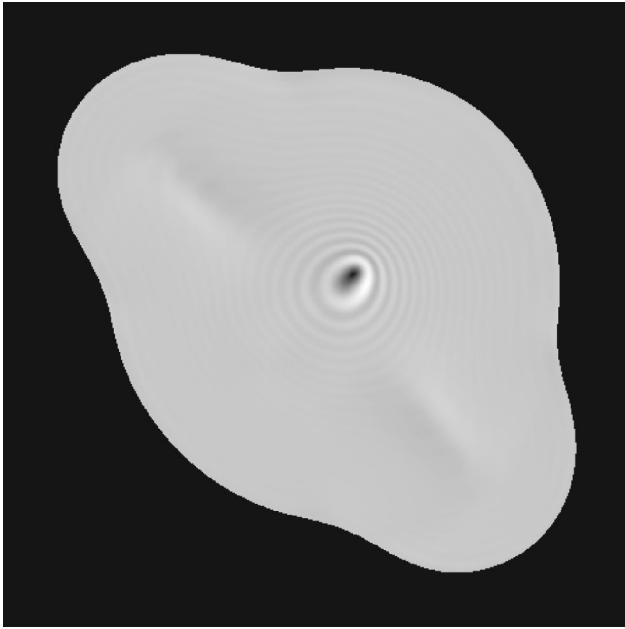
Fig. 6.   Relative magnitude of the vortex-operator-derived magnitude.   Gray-scale encoding means that black represents zero and white represents peak value.   Central region values vary from 0.16 to 1.30, with most regions near the ideal value of 1.00.

So, in general, we can say that the amplitude of $[\check{P}_k(\check{u}_s, \check{v}_s)]_n$ is different from our first stationary phase expansion by an amount that depends upon the second-order derivatives of both the underlying phase and the orientational phase.   This is broadly consistent with initial simulations of 2-D demodulation using the spiral phase quadrature operator.[1]   The relative error in the local Hessian is as follows:

$$\frac{\Delta H}{H}$$

$$= \frac{(\beta_{2,0}\beta_{0,2} - \beta_{1,1}^2) - (\psi_{0,2}\beta_{2,0} + \psi_{2,0}\beta_{0,2} - 2\psi_{1,1}\beta_{1,1})}{\psi_{2,0}\psi_{0,2} - \psi_{1,1}^2}.$$

$$(53)$$

There are a variety of situations where the relative error is zero, the simplest being when the orientation is locally linear ($\beta_{2,0} = \beta_{0,2} = \beta_{1,1} = 0$), corresponding to the simple case of straight fringes.   The detailed analysis of the amplitude error propagation will not be pursued further in this preliminary investigation.   Figure 6 shows a gray-scale representation of the actual amplitude error calculated for the vortex operator demodulation.   The main errors are constrained to the center of the fringe pattern.   The center of the fringe pattern also corresponds to a region where the orientation components [defined in Eqs. (47)] are singular ($\psi_{1,0}^2 + \psi_{0,1}^2 = 0$).

It is worth noting that, given sufficient *a priori* information, it is conceivable that error-correcting schemes could be devised utilizing the above error estimates.

7. CONCLUSION

The validity of the intuitively inspired spiral phase quadrature transform has been confirmed by using the method of stationary phase.   We have shown, in the asymptotic limit, that taking a quadrature fringe pattern and multiplying it by an orientational phase pattern followed by Fourier transformation gives the same result as that of Fourier-transforming a fringe pattern and then multiplying by a spiral phase factor.   Using an alternative formulation of the stationary phase method, we have shown how phase errors arise when the radius of curvature of the fringe pattern is small (curvature large) compared with the fringe spacing.   Amplitude errors in the spiral phase transform are related to more complicated combinations of second- and higher-order derivatives of the phase function underlying the fringe pattern.   We have established a theoretical basis for further developments in direct, two-dimensional fringe demodulation and analysis.

APPENDIX A: PRACTICAL ASPECTS OF THE FRINGE ORIENTATIONAL FACTOR

The correct functioning of the vortex transform depends upon the correct definition and evaluation of the orientation angle $\beta(x, y)$.   For a complex function the definition follows simply from the phase gradient.   For real fringes there is always an ambiguity that is due to a loss in some sign information, as shown by

$$\cos(\psi) = \cos(-\psi).$$

$$(A1)$$

This sign ambiguity is well-known in interferometry (e.g., see Kreis[21]).   There is a significant advantage that emerges from the vortex transformation approach to fringe demodulation.   The advantage is that the ambiguity resides purely in the choice of sign for the fringe orientation because the fundamental quadrature operation has been performed already by the spiral phase Fourier multiplier.   Now the underlying assumption in this work is that we are dealing with (open or closed) fringe patterns with smooth and infinitely differentiable amplitude and phase parameters.   This means that the fringe orientation is everywhere smooth and differentiable, except at special points, where the phase gradient is identically zero and the orientation is undefined.   Interestingly, these points give rise to spiral phase singularities in the orientation phase factor $\exp(-i\beta)$, evoking the concept of ever-decreasing spirals.   Singularities in the orientation can occur only at points where $\nabla\psi = 0$, points that have a stationary phase Fourier component at zero frequency ($u_s = v_s = 0$), which is the one frequency where the spiral phase factor is effectively undefined.   (If we consider its value as the average of its limiting value as we approach the origin from different directions, then the modulus is zero and the phase is undefined.)   In general, these singular points of orientation will have problematic expansions in terms of conventional power series.

Another problem with evaluation of the fringe orientation is the effect of amplitude modulation on the phase gradient estimate.   In general, the amplitude modulation is unknown *a priori*, leading to a signal gradient ∇f that deviates from the phase gradient $\nabla\psi$:

$$\nabla f = \nabla b[\cos(\psi)] - \nabla\psi[b \sin(\psi)].$$

$$(A2)$$

The error in the estimated orientation is then ϵ, where

$$\tan(\beta_{\text{est}}) = \tan(\beta + \epsilon) = \frac{f_{0,1}}{f_{1,0}}$$

$$= \frac{\psi_{0,1} b \sin(\psi) - b_{0,1} \cos(\psi)}{\psi_{1,0} b \sin(\psi) - b_{1,0} \cos(\psi)}. \qquad (A3)$$

And it can be shown that

$$\tan(\epsilon)$$

$$= \frac{(\psi_{0,1} b_{1,0} - \psi_{1,0} b_{0,1}) \cos(\psi)}{(\psi_{0,1}^2 + \psi_{1,0}^2) b \sin(\psi) - (\psi_{1,0} b_{10} + \psi_{0,1} b_{0,1}) \cos(\psi)}, \qquad (A4)$$

which means that the orientation error is always zero at zero crossings of f [i.e., $\cos(\psi) = 0$] and at regions where the amplitude gradient either is zero or is in the same direction (mod π) as that of the phase gradient:

$$\frac{b_{0,1}}{b_{1,0}} = \frac{\psi_{0,1}}{\psi_{1,0}} \equiv \tan(\beta). \qquad (A5)$$

In other situations the error is nonzero. In Paper I [Ref. 1, relations (28) and (30) and Eq. (31)], we showed that errors in the estimated orientation produce second-order errors in the vortex-operator-based phase demodulation. In other words, the overall method is inherently robust to small orientation errors.

Finally, a few observations will be made about practical schemes for estimating the orientation mod 2π, as required by our spiral phase demodulation method. The first point to note is that simple gradient-based schemes suffer from sign flips that occur in every period of a real fringe pattern. If we are given the complex fringe pattern, then we can easily estimate the gradient:

$$\nabla\{\exp(i\psi)\} = \exp(i\psi)\nabla\psi. \qquad (A6)$$

If we are just given the cosine component, then

$$\nabla\{\cos(\psi)\} = -\sin(\psi)\nabla\psi. \qquad (A7)$$

We then estimate the actual angle from an arctangent of the gradient components:

$$\beta = \arctan\left[\frac{-\psi_{0,1}\sin(\psi)}{-\psi_{1,0}\sin(\psi)}\right]. \qquad (A8)$$

The problem here is that the sine components do not simply cancel out, because the arctangent quadrants flip polarity in synchrony with the sine polarity. The same problem arises if we use the spiral phase transform itself to estimate the orientation:

$$i\exp(i\beta) b \sin(\psi) \sim \mathcal{F}^{-1}\{\exp(i\phi)\mathcal{F}\{b\cos(\psi)\}\}, \quad (A9)$$

$$\arg\{i\exp(i\beta) b \sin(\psi)\} = \arctan\left[\frac{\cos(\beta)\sin(\psi)}{-\sin(\beta)\sin(\psi)}\right], \qquad (A10)$$

where the $\sin(\psi)$ multiplier introduces an ambiguity in the tangent quadrants again. There is also another (related) insidious problem with gradient-based orientation estimation that occurs when the sine component approaches zero [$\sin(\psi) \to 0 \Leftrightarrow \cos(\psi) \to$ extremum] and the practical orientation estimate becomes noise sensitive. Although we do not consider practical aspects of

noise analysis in this publication, it is clear that an orientation estimate that is independent of the value of $\sin(\psi)$ is desirable. We could use second derivatives of the fringe pattern, which are related to the value of $\cos(\psi)$. By combining both $\sin(\psi)$ and $\cos(\psi)$ factors, one can obtain uniform (i.e., independent of ψ) estimates of the orientation. No more of the details will be said here—as the subject warrants a paper on its own—except to say that methods based upon the energy operator[22,23] or tensor analysis[20] are recommended. In either case the estimate of the orientation always occurs in a quadratic form, i.e., $\exp(2i\beta)$. This is really just another incarnation of the sign ambiguity:

$$[\exp(i\beta)]_{\text{est}} = \pm\sqrt{\exp(2i\beta)}. \qquad (A11)$$

Perhaps the easiest way (while not forgetting that there are other methods) to obtain the final result that we require (orientation estimate mod 2π) is to unwrap 2β mod 4π and then halve it. Remember that the unwrapping is relatively straightforward because the underlying assumption is for a smoothly varying phase and hence a smoothly varying orientation (except at the centers of closed curves, as discussed above). Figure 3(a) shows an orientation phase map ($+\sqrt{\exp(2i\beta)}$) that has not been unwrapped, while Fig. 3(b) shows a correctly unwrapped $[\exp(i\beta)]$ map. Note that Fig. 3(a) still contains a second-order spiral phase discontinuity, and Fig. 3(b) a first-order spiral phase discontinuity. The discontinuities are merely manifestations of the undefined orientation at the center of curvature of a closed fringe pattern.

ACKNOWLEDGMENTS

Address correspondence to Kieran G. Larkin at the second location given on the title page or by e-mail, kieran@research.canon.com.au.

REFERENCES AND NOTES

1. K. G. Larkin, D. Bone, and M. A. Oldfield, "Natural demodulation of two-dimensional fringe patterns. I. General background of the spiral phase quadrature transform," J. Opt. Soc. Am. A **18**, 1862–1870 (2001).
2. Z. Jaroszewicz, A. Kolodziejczyk, D. Mouriz, and S. Bara, "Analytic design of computer-generated Fourier-transform holograms for plane curves reconstruction," J. Opt. Soc. Am. A **8**, 559–565 (1991).
3. M. A. Stuff and J. N. Cederquist, "Coordinate transformations realizable with multiple holographic optical elements," J. Opt. Soc. Am. A **7**, 977–981 (1990).

4. R. N. Bracewell, *The Fourier Transform and Its Applications* (McGraw-Hill, New York, 1978).

5. According to Bracewell (Ref. 4, p. 83), Lerch's theorem states that if two functions $f(x, y)$ and $g(x, y)$ have the same Fourier transform, then $f(x, y) - g(x, y)$ is a null function.

6. There are a number of ways to remove the offset. Low-pass filtering is the simplest but often not the best method. In situations with multiple phase-shifted interferograms, the difference between any two frames will have the offset nullified. Adaptive filtering methods can also provide more accurate offset removal. In practice, offset removal may be difficult. The difficulty exists even for 1-D signal demodulation using Hilbert techniques, as shown in detail by N. E. Huang, Z. Shen, S. Long, M. C. Wu, H. H. Shih, Q. Zheng, N. Yen, C. C. Tung, and H. H. Liu, "The empirical mode decomposition and the Hilbert spectrum for nonlinear and nonstationary time series analysis," Proc. R. Soc. London Ser. A **454**, 903–995 (1998). We shall not discuss the difficulty further in this initial exposition, but it should be noted that failure to remove the offset signal correctly will introduce significant errors.

7. A. H. Nuttall, "On the quadrature approximation to the Hilbert transform of modulated signals," Proc. IEEE **54**, 1458–1459 (1966).

8. M. Takeda, H. Ina, and S. Kobayashi, "Fourier-transform method of fringe-pattern analysis for computer-based topography and interferometry," J. Opt. Soc. Am. **72**, 156–160 (1982).

9. D. J. Bone, H.-A. Bachor, and R. J. Sandeman, "Fringe-pattern analysis using a 2-D Fourier transform," Appl. Opt. **25**, 1653–1660 (1986).

10. J. L. Marroquin, J. E. Figueroa, and M. Servin, "Robust quadrature filters," J. Opt. Soc. Am. A **14**, 779–791 (1997).

11. N. Bleistein and R. A. Handelsman, *Asymptotic Expansion of Integrals* (Dover, New York, 1975).

12. We shall refrain from calling this function the 2-D analytic signal at present because there are several conflicting definitions of analyticity [13] in multiple dimensions. The alternative term "monogenic" does not seem appropriate because

the word now has another widespread use in molecular genetics.

13. M. A. Fiddy, "The role of analyticity in image recovery," in *Image Recovery: Theory and Application*, H. Stark, ed. (Academic, Orlando, Fla., 1987).

14. J. J. Stamnes, *Waves in Focal Regions* (Hilger, Bristol, UK, 1986).

15. The Gaussian curvature C at a critical point (zero gradient) is equal to the Hessian;

$$C = \frac{\psi_{2,0}\psi_{0,2} - \psi_{1,1}^2}{(1 + \psi_{1,0}^2 + \psi_{0,1}^2)^{3/2}} = \frac{H}{(1 + \psi_{1,0}^2 + \psi_{0,1}^2)^{3/2}},$$

$$\psi_{1,0} = \psi_{0,1} = 0 \Rightarrow C = H.$$

16. A. Papoulis, *Systems and Transforms with Applications in Optics* (McGraw-Hill, New York, 1968).

17. A zero gradient of the orientation implies a zero Hessian. The converse is not true, as there are surfaces, such as the cone, with a zero Hessian and a nonzero orientation gradient.

18. J. F. Nye, *Natural Focusing and the Fine Structure of Light* (Institute of Physics, Bristol, UK, 1999).

19. K. G. Larkin and B. F. Oreb, "Propagation of errors in different phase-shifting algorithms: a special property of the arctangent function," in *Interferometry: Techniques and Analysis*, G. M. Brown, O. Y. Kwon, M. Kujawinska, and G. T. Reid, eds., Proc. SPIE **1755**, 219–227 (1992).

20. G. H. Granlund and H. Knutsson, *Signal Processing for Computer Vision* (Kluwer Academic, Dordrecht, the Netherlands, 1995).

21. T. Kreis, *Holographic Interferometry. Principles and Methods* (Akademie, Berlin, 1996), Vol. 1.

22. J. F. Kaiser, "On a simple algorithm to calculate the 'energy' of a signal," in *Proceedings of the IEEE International Conference on Acoustics, Speech, and Signal Processing* (IEEE, New York, 1990), pp. 381–384.

23. P. Maragos, A. C. Bovik, and T. F. Quatieri, "A multidimensional energy operator for image processing," in *Visual Communications and Image Processing '92*, P. Maragos, ed., Proc. SPIE **1818**, 177–186 (1992).